Supporting material for:

Measurement of effective wetting area at hydrophobic solid–liquid interface

Dejian Zhang[1], Satoko Takase[2], Gyoko Nagayama[1]*

[1]Department of Mechanical Engineering, Kyushu Institute of Technology, Sensui 1-1, Tobata, Kitakyushu, Fukuoka 804-8550, Japan

[2]Department of Chemical Engineering, Kyushu Institute of Technology, Sensui 1-1, Tobata, Kitakyushu, Fukuoka 804-8550, Japan

Corresponding Author:

Gyoko Nagayama

Email: nagayama.gyoko725@mail.kyutech.jp

1. Water contact angle measurement system and measurement cell

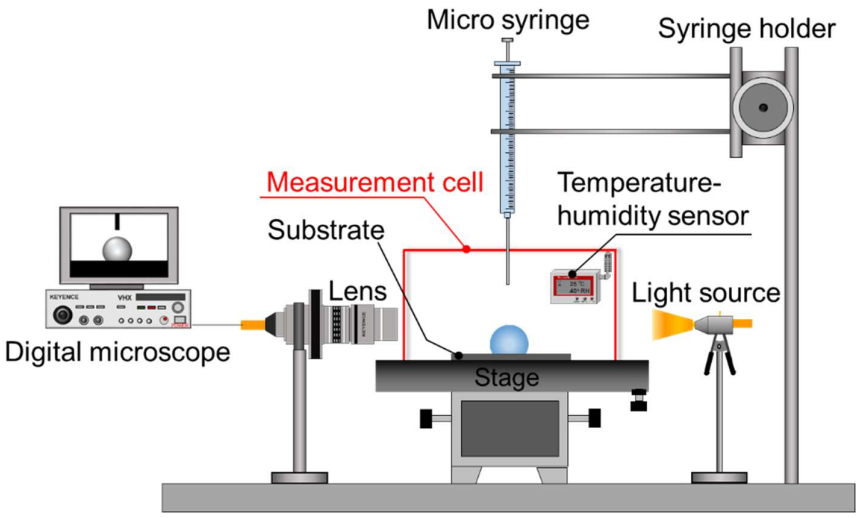

Fig. s1. Schematics of contact angle measurement system and measurement cell.

2. Experimental method on the measurement of water contact angle at patterned Si surface.

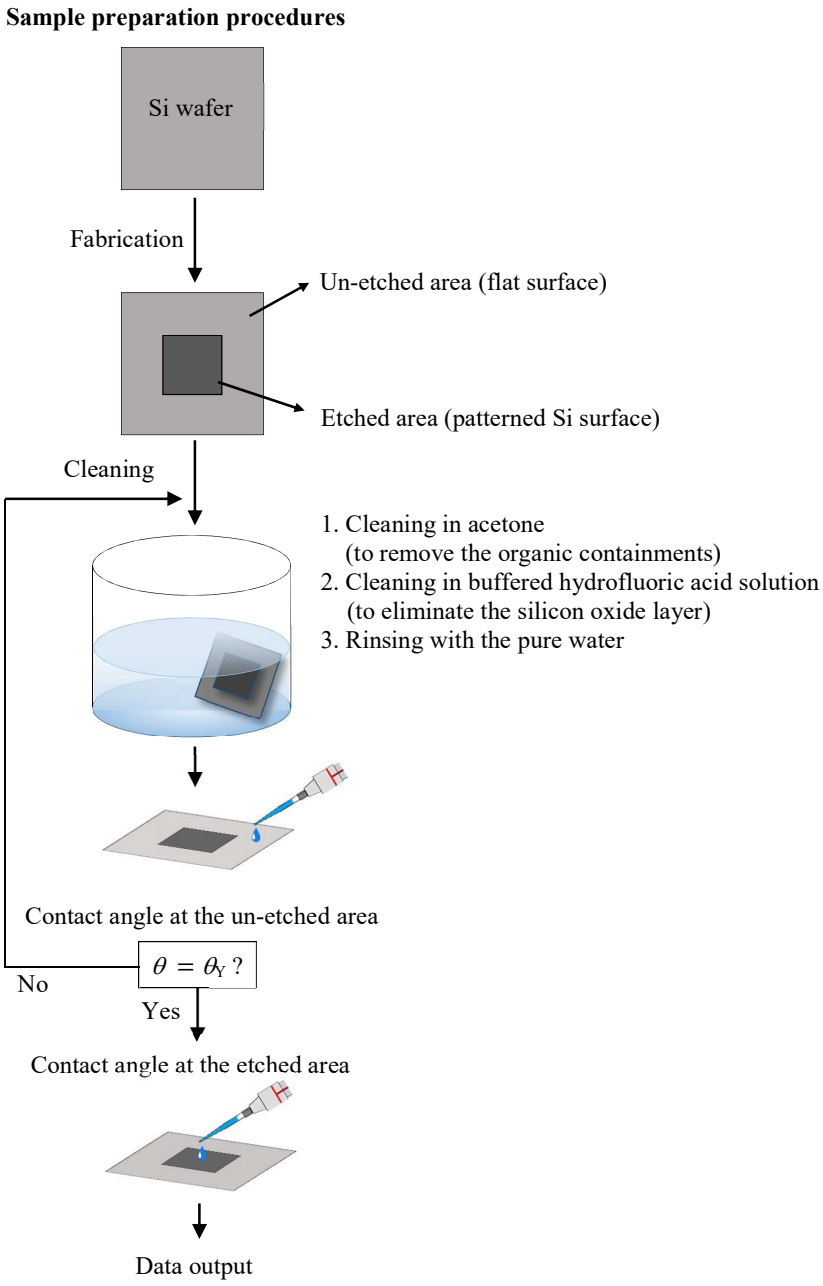

Fig. s2. Schematic diagram of sample preparation and contact angle measurement.

3. Electrochemical impedance measurement system

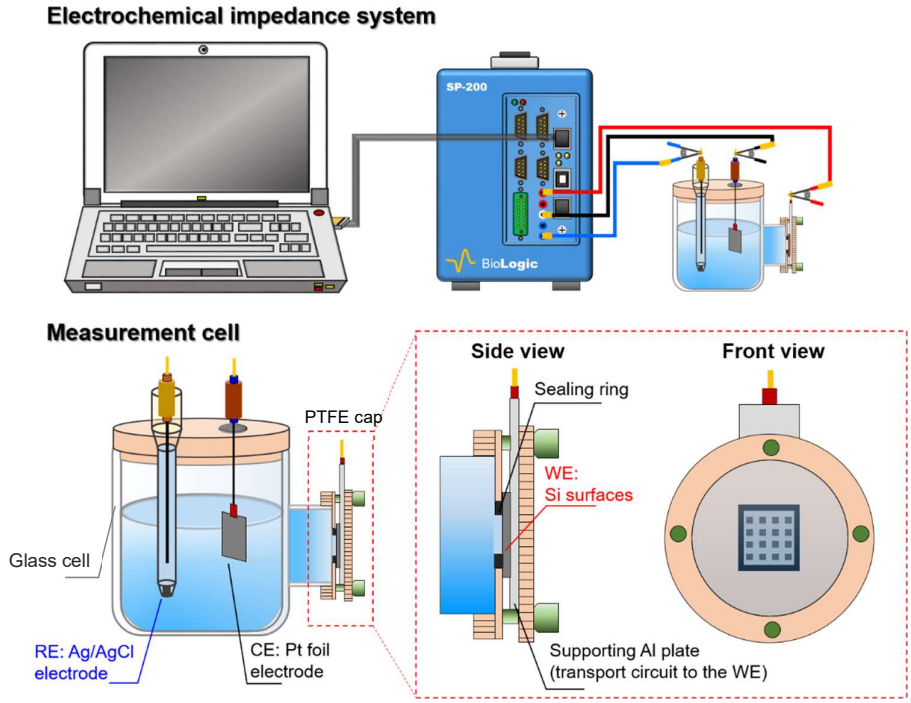

Fig. s3. Schematics of electrochemical impedance measurement system and measurement cell.

4. Comparison of WCAs between pure water and electrolyte droplets on Si surfaces.

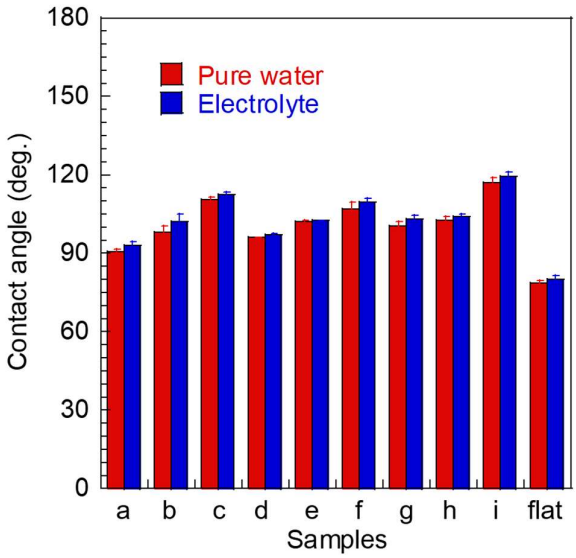

Fig. s4. Comparison of WCAs between pure water and electrolyte droplets on Si surfaces.

Table s1. The measured WCAs of pure water and electrolyte droplets on patterned Si surfaces.

Samples	Pure water WCA (deg.)	Electrolyte WCA (deg.)
a	90.6 ± 1.2	93.0 ± 1.7
b	98.0 ± 2.3	102.1 ± 2.9
c	110.7 ± 0.6	112.4 ± 1.2
d	96.1 ± 0.0	97.0 ± 0.7
e	102.1 ± 0.4	102.5 ± 0.3
f	107.1 ± 2.3	109.4 ± 1.6
g	100.6 ± 1.3	102.9 ± 1.6
h	102.6 ± 1.3	104.0 ± 1.0
i	116.8 ± 2.3	119.3 ± 1.8
flat Si	78.6 ± 1.0	79.8 ± 1.7

5. Structural parameters and experimental WCA results.

Table s2. The measured and designed structural parameters, as well as the experimental WCAs of the patterned Si surfaces.

	Measurement (μm)					Original design (μm)					WCA
	a	*b*	*s*	*Φ*	r_w	*a*	*b*	*s*	*Φ*	r_w	(deg.)
a	3.5	4.6	8.1	0.81	1.14	3.0	5.0	8.0	0.86	1.10	90.6 ± 1.2
b	4.5	3.7	8.2	0.70	1.22	4.0	4.0	8.0	0.75	1.18	98.0 ± 2.3
c	5.7	2.4	8.1	0.50	1.36	5.0	3.0	8.0	0.61	1.29	110.7±0.6
d	5.4	4.8	10.2	0.72	1.21	5.0	5.0	10.0	0.75	1.18	96.1 ± 0.1
e	6.6	3.7	10.3	0.59	1.30	6.0	4.0	10.0	0.64	1.26	102.1±0.4
f	8.0	2.4	10.4	0.41	1.43	7.0	3.0	10.0	0.51	1.36	107.1±2.3
g	9.0	6.4	15.4	0.66	1.25	8.0	7.0	15.0	0.72	1.21	100.6±1.3
h	11.1	4.5	15.6	0.49	1.37	10.0	5.0	15.0	0.56	1.33	102.6±1.3
i	12.0	3.0	15.0	0.36	1.47	12.0	3.0	15.0	0.36	1.47	116.8±2.3
flat	-	-	-	1.00	1.00	-	-	-	1.00	1.00	78.6 ± 1.0

6. Fractal dimension D

The fractal dimension analysis of the patterned Si surfaces is based on the traditional box counting method for the 2D confocal laser scanning microscope images. With the aid of fractal analysis software [http://cse.naro.affrc.go.jp/sasaki/fractal/fractal.html, fractal3, Ver. 3.4.7], the fractal dimension D is obtained from the gray scale images by box counting method defined as

$$\mathrm{D} = \frac{\log_{10} N}{\log_{10} \delta} \tag{s1}$$

where N is the number of boxes that cover the surface, and δ is the magnification (i.e. the inverse of the box size). Fig. s5 shows the analyzed surface images and the results of Eq. (s1) to calculate the fractal dimensions at patterned Si surfaces. The details of the individual fractal dimension for the 9 patterned Si samples are summarized in the Table s3. The mean fractal dimension is 2.24 and the standard deviation of the fractal dimension is 0.06.

Table s3. Fractal dimension D of patterned Si surfaces.

Sample a	2.21 ± 0.02
Sample b	2.23 ± 0.06
Sample c	2.32 ± 0.06
Sample d	2.14 ± 0.03
Sample e	2.28 ± 0.02
Sample f	2.29 ± 0.02
Sample g	2.20 ± 0.02
Sample h	2.17 ± 0.06
Sample i	2.30 ± 0.11
Flat Si	2.00

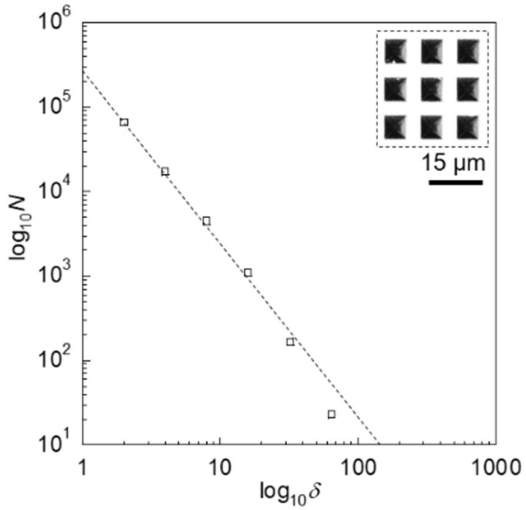

Fig. s5. An example of fractal dimension analysis based on box counting method for patterned Si surface of $\Phi = 0.59$.

7. Nyquist plots for patterned Si surfaces

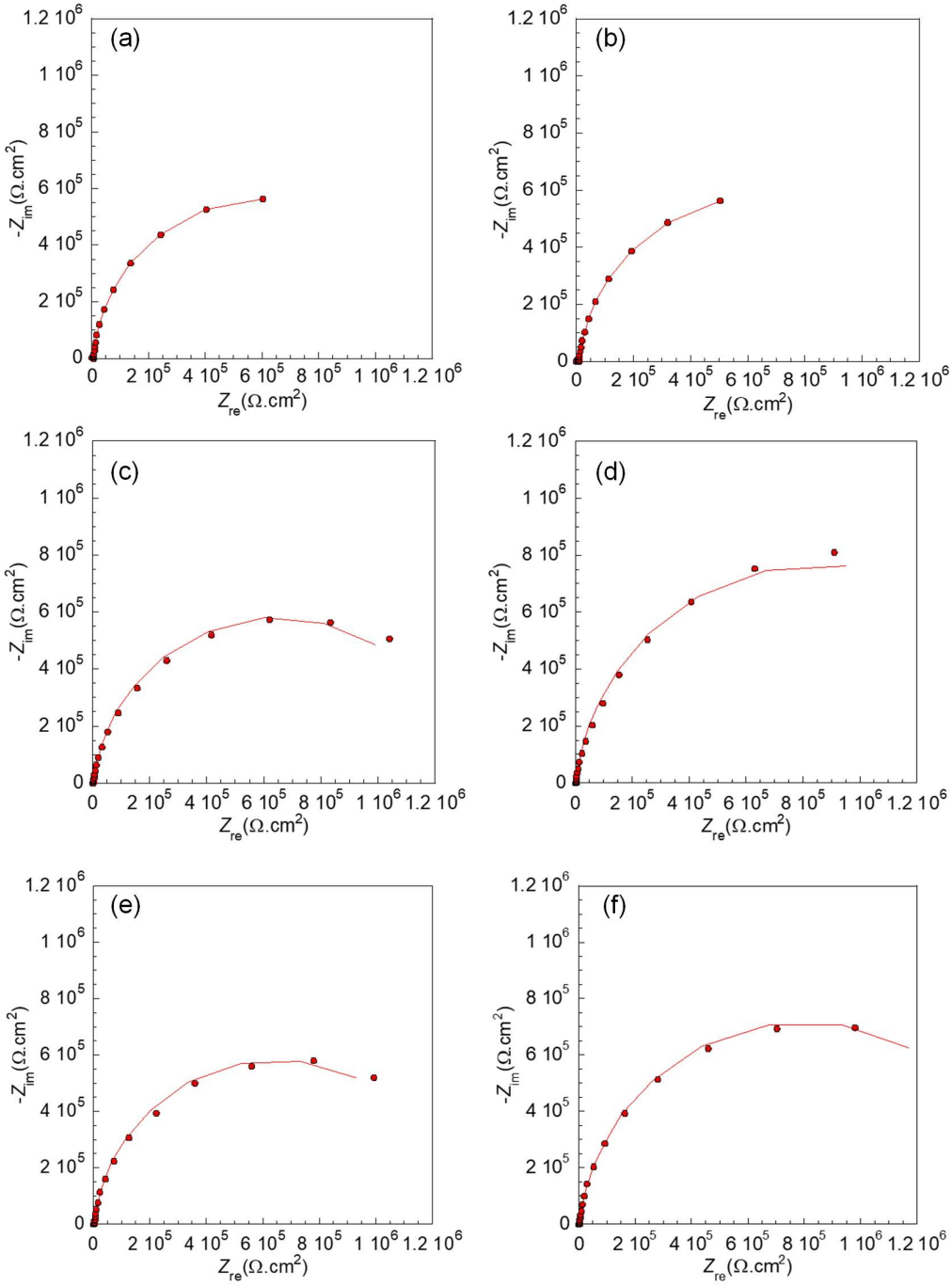

Fig. s6. Nyquist plots for Si surfaces with WCAs of (a) 107.1°, (b) 102.6°, (c) 98.0°, (d) 110.7°, (e) 96.1°, and (f) 100.6° in 3.5 wt% NaCl solution. Symbols are measured results and lines are corresponding fitted curves.

8. Schematic of pressure on solid–liquid interface.

The measurement of impedance is performed by immersing Si surface in the electrolyte (Fig. s7b), while the wettability measurement is performed under atmosphere (Fig. s7a). Lafuma et al. found that the water contact angle of a droplet sandwiched by two parallel plates decreased from 165° to 145° with increasing the imposed pressure from 50 Pa to 250 Pa, corresponding to the wetting transition from Cassie regime to Wenzel regime *(Lafuma, A., & Quéré, D., Nature materials, 2003)*. That is, the effective wetting area will increase due to the wetting transition (caused by the imposed pressure). In our experiment, the mean hydrostatic pressure P acted to the Si surfaces corresponding to a fixed immersing height h=1.5 cm is approximately to

$$P = \rho gh \approx 1000kg/m^3 \times 9.8m/s^2 \times 1.5cm = 147Pa$$

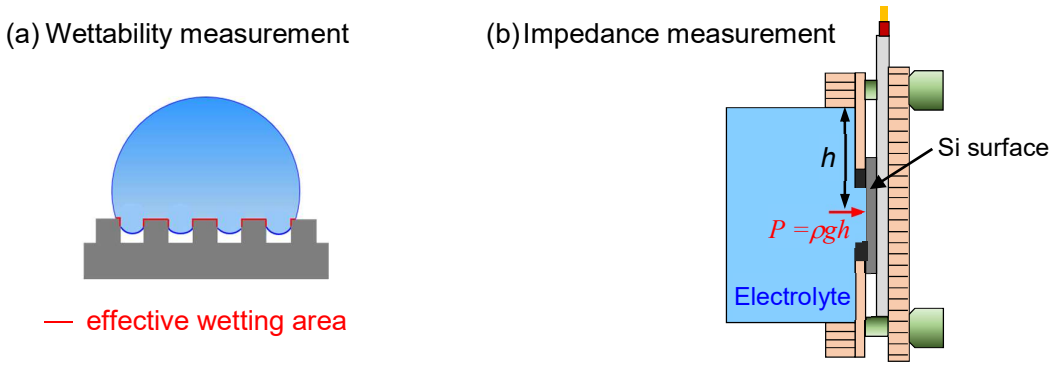

Fig. s7. Schematic of pressure works on the effective wetting area.

9. Deviations of effective wetting area.

The deviations of A_{ew}/A_0 (Eq. 9) and A_{ew}/A_0 (Eq. 7) shown in Table 2 are calculated based on the deviations of water contact angles and the deviations between experimental and fitted data of interface impedance Z, respectively.

Table s4. The measured WCAs of pure water and electrolyte droplets on patterned Si surfaces.

Samples	Water contact angle (deg.)	Interfacial resistance Z ($\Omega.cm^2$)
a	90.6 (0.013)	1.17×10^6 (4.343)
b	98.0 (0.024)	1.30×10^6 (7.261)
c	110.7 (0.006)	1.72×10^6 (4.264)
d	96.1 (0.001)	1.30×10^6 (15.28)
e	102.1 (0.004)	1.41×10^6 (7.982)
f	107.1 (0.021)	1.31×10^6 (1.228)
g	100.6 (0.013)	1.60×10^6 (14.83)
h	102.6 (0.013)	1.30×10^6 (4.417)
i	116.8 (0.019)	1.76×10^6 (3.742)
flat Si	78.6 (0.013)	1.08×10^6 (2.906)

The values presented in parenthesis are deviations (%).

10. The effective wetting area estimated based on the measured WCA and classical wetting models (Cassie–Baxter model and Wenzel model).

In order to further verify the wetting state of the patterned Si surfaces is intermediate wetting state (i.e. partial wetting model). We also compared the A_{ew}/A_0 on condition of that the wetting state is Cassie–Baxter state or Wenzel state.

Suppose the wetting state of the patterned Si surfaces is Cassie–Baxter state. Based on the Cassie–Baxter model (Eq. 4), A_{ew}/A_0 can be calculated by substituting the measured WCA θ_Y and θ_C, as shown in the following:

$$A_{ew} / A_0 = \frac{\cos\theta_C + 1}{1 + \cos\theta_Y} \tag{s2}$$

On the other hand, suppose the wetting state of the patterned Si surfaces is Wenzel state. The A_{ew}/A_0 can be obtained based on the Wenzel model (Eq. 3), measured θ_Y and θ_W, which is expressed as:

$$A_{ew} / A_0 = \frac{\cos\theta_W}{\cos\theta_Y} \tag{s3}$$

The effective wetting area ratio A_{ew}/A_0 evaluated from the wettability (Eq. s2 and Eq. s3) and electrochemical impedance (Eq. 7) results are summarized in Table s5 and the comparisons are shown in Fig. s8. Compare with A_{ew}/A_0 evaluated from impedance results, the A_{ew}/A_0 evaluated from Eq. 9 (Fig. 10) show better correspondence than that from Eq. s2 and Eq. s3 (Fig. s8), indicating the partial wetting model is more suitable to describe the wetting state of patterned Si surfaces.

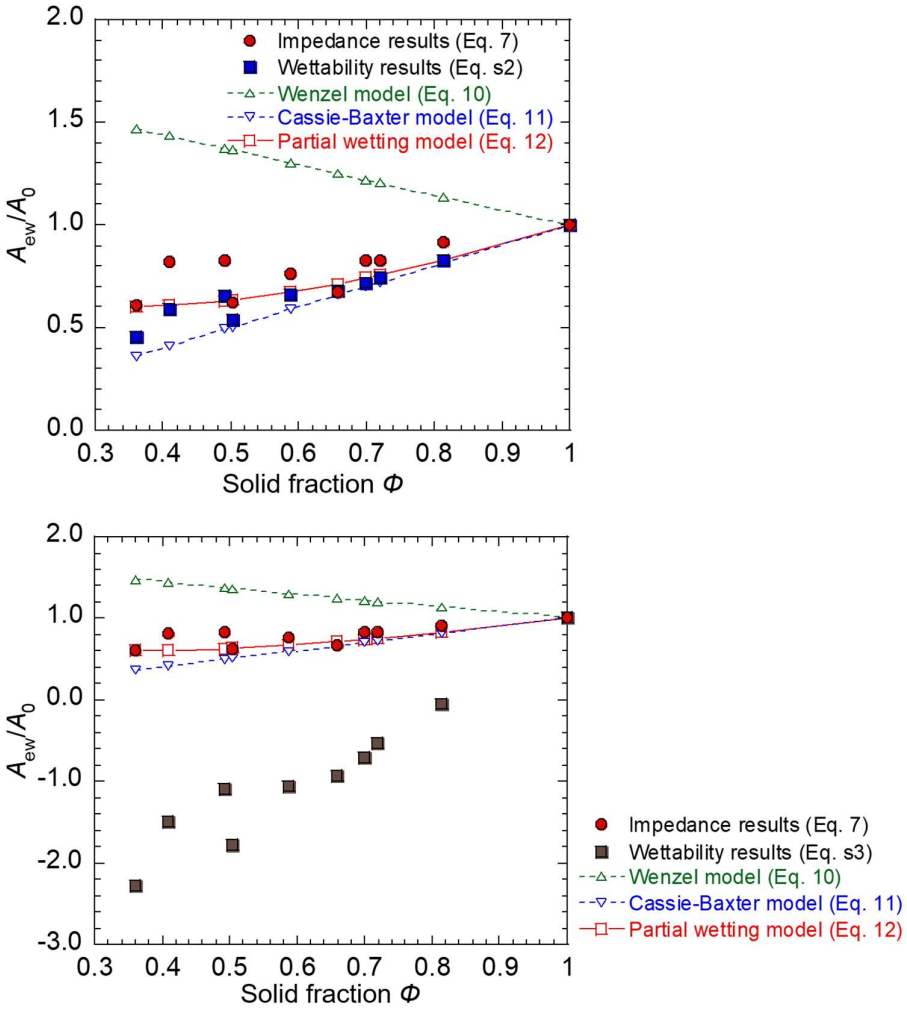

Fig. s8. Comparisons of A_{ew}/A_0 between experiments and theoretical models.

Table s5. Effective wetting area evaluated from wettability results (Eq. s2 and Eq. s3).

WCA (deg.)	A_{ew}/A_0 (Eq. s2)	A_{ew}/A_0 (Eq. s3)
90.6	0.827	-0.050
98.0	0.718	-0.705
110.7	0.540	-1.789
96.1	0.746	-0.538
102.1	0.660	-1.062
107.1	0.589	-1.488
100.6	0.681	-0.933
102.6	0.654	-1.099
116.8	0.459	-2.280
78.6	1.000	1.000